JOURNAL OF OPTOELECTRONİCS AND ADVANCED MATERİALS Vol. 9, No. 7, July 2007, p. 2217 - 2226

Some physical properties of ultrasonically sprayed tin oxide films: the effect of the substrate temperature

F. ATAY, M. DEMIR, S. KOSE, V. BILGIN, I. AKYUZ
Department of Physics, Eskisehir Osmangazi University, 26480 Eskisehir, Turkey

In this work, SnO_2 films, belonging to the transparent conducting oxides family and commonly used in photovoltaic solar cells and opto-electronic devices, were deposited by ultrasonic spray pyrolysis technique onto glass substrates at different substrate temperatures of 200, 250, 300 and 350±5°C. The effect of the substrate temperature on the structural, surface, optical and electrical properties of the produced films was investigated. The structural properties such as crystallinity level, grain size and half peak width were analyzed by using x-ray diffraction patterns. The surface properties and elemental distributions were characterized using scanning electron microscopy and energy dispersive x-ray spectroscopy, respectively. The optical properties like transmission, reflection, absorption and refractive index were investigated depending on the substrate temperature, and the optical band gaps were calculated using optical method. The electrical conduction mechanisms of the films were investigated using current voltage characteristics and the electrical conductivities were calculated with two-probe technique. Also, the energies of donors and donor-like traps were determined from lnσ~1000/T graphs. After all investigations, it was determined that the structural, optical, electrical and surface properties strongly depend on the substrate temperature, and especially SnO_2 films obtained at a substrate temperature of 250 ± 5°C have desired characteristics for solar cell applications.

(Received January 16, 2007; accepted June 27, 2007)

Keywords: SnO_2 films; Ultrasonic spray pyrolysis; Electrical, optical and structural properties, SEM, EDS

1. Introduction

SnO_2 films which belong to IV-VI compound semiconductors have a wide band gap (E_g~3.6-4.0 eV) at room temperature and n-type electrical conductivity [1-4]. These films have tetragonal crystal system, and lattice parameters are a=4.737 Å and c=3.186 Å [5, 6]. SnO_2 films have low electrical resistivity (10^{-2}-10^{-4} Ω.cm), high transparency (%70-85) in visible region and high chemical, thermal and mechanical stability [7-11]. These electro-optical properties make SnO_2 films common materials for photovoltaic solar cells, thin film resistors, electroluminescence circuits, liquid crystal displays, detectors and gas sensors [12-17]. SnO_2 in various forms (such as bulk, thick and thin films) has been investigated for sensing a number of gases such as CO, NO_2, NH_3, CH_4 and alcohol vapors [18]. Transparent conductive SnO_2 thin films have been widely used as transparent electrodes in electronic devices [19]. Selective electrical conductivity, high thermal and chemical stability, easy and low cost fabrication are the causes of widespread applications of SnO_2 as gas sensor [20, 21].

SnO_2 thin films are produced by different techniques such as thermal evaporation, sputtering, spray pyrolysis, sol-gel and hydrothermal [22-24]. Among these techniques, spray pyrolysis is an economic and simple technique and allows film deposition on large areas. The films produced by this technique have polycrystalline structure [25-30]. Ultrasonic spray pyrolysis (USP) technique includes an ultrasonic atomizer which is connected to an oscillator. This ensures the solution to be sprayed with a better atomizing using ultrasonic waves and this results in decreasing of droplet size and production of more homogeneous materials [31, 32].

The aim of this work is to investigate the effect of substrate temperature on the structural, optical, electrical and surface properties of SnO_2 films produced by USP technique.

2. Experimental details

SnO_2 films were deposited onto glass substrates (1×1 cm^2) by USP technique at the substrate temperatures of 200, 250, 300 and 350±5 °C, and the films were named as M1, M2, M3 and M4 depending on the increasing substrate temperature. Details of the USP technique were given in our previous works [33-35]. The ultrasonic frequency is used is 100 kHz, and the droplet size is 20 μm. The spraying solution contains 0.05 M $SnCl_2.2H_2O$ salt. The volume of the spraying solution was 125 ml, and the solution was sprayed during 25 mins. The solution flow rate was controlled by a flowmeter and kept at 5 $ml.min^{-1}$. Nitrogen gas was used as the carrier gas (0.2 $kg.cm^{-2}$). The glass substrates were heated by an electrical heater and the substrate temperature was measured using an iron-constantan thermocouple.

The thicknesses of SnO_2 films which are obtained at the substrate temperature of 200±5 °C were measured as 4.0 μm, using Elcometer 345 Digital Coating Thickness gauge. However, the thickness is so thick for photovoltaic applications. To reduce the film thicknesses, the substrate

temperature was increased, and the thicknesses of SnO_2 films which are obtained at the substrate temperature of 250, 300 and 350±5 °C were measured as 3.57, 2.00 and 1.66 μm, respectively. So, it was seen that the thicknesses of the films decrease depending on the substrate temperature. We think that this variation resulted from the evaporation of atomized particles just before they reach to the substrate. The structural properties of all films were studied by an x-ray diffractometer (Rigaku Model, λ= 1.5405 Å) with CuK_α radiation. Optical transmissions and absorbances of the films were recorded with a Unicam 2-UV spectrophotometer. Electrical contacts were made by touching the platinum tips on the surface of the films. Current-voltage (I-V) measurements were done in dark by using Keithley 6487 Picoammeter/Voltage Source. The conductivity-temperature measurements (10-320 K) were made using a cryostat, equipped by a Lake Shore 332 Temperature Controller and Keithley 6487 Picoammeter/Voltage Source. The surface properties of all films were investigated using a Zeiss Supra 50VP scanning electron microscope (SEM). The elemental analyses of the films were performed by energy dispersive x-ray spectroscopy (EDS).

3. Results and discussion

3.1 Structural properties

The XRD patterns ($20° \leq 2\theta \leq 100°$) of SnO_2 films are shown in Fig. 1. It was determined that M1-M4 films have polycrystalline structures and tetragonal SnO_2 crystal systems. The preferential orientations of the films were determined by using the texture coefficient TC(hkl) [36]. Thus, it was seen that the preferential orientations of M1 and M2 films are in the (110) direction, while those of the M3 and M4 films are (211). Also, it was determined that peak intensities of M3 and M4 films increased, while those of the M2 films decreased as compared to M1 films. Furthermore, it was stated that background intensities of M3 and M4 films decreased, and those of the M2 films increased as to M1 films. Besides, the full width half maximums (FWHM, B) decreased by increasing substrate temperature. Thus, it was determined that the crystallinity levels of the SnO_2 films improved at high substrate temperature depositions (especially 300 and 350±5 °C). So, it was concluded that M2 films have a little bad crystallization according to other films. Lattice constants of M1-M4 films were calculated for the peaks related to the preferential orientations. These values with the ones taken from American Society for Testing Materials (ASTM) cards are given in Table 1. It was determined that these values are in good agreement. Besides, the grain sizes of the films were determined for preferential orientations by using the classical Scherrer Formula [37, 38], assuming that microstrain can be neglected. The grain sizes (t) and half peak widths (B) of all films are given in Table 2. Also, the plots of B and t vs. substrate temperature are shown in Fig. 2. It was determined from Table 2. and Fig. 2. that B values of SnO_2 films decreased and t values increased with increasing substrate temperature. So, it can be concluded that the substrate temperature has a strong effect on the structural properties, and the crystallinity levels of SnO_2 films improves with increasing substrate temperature (specially 300 and 350 ± 5 °C).

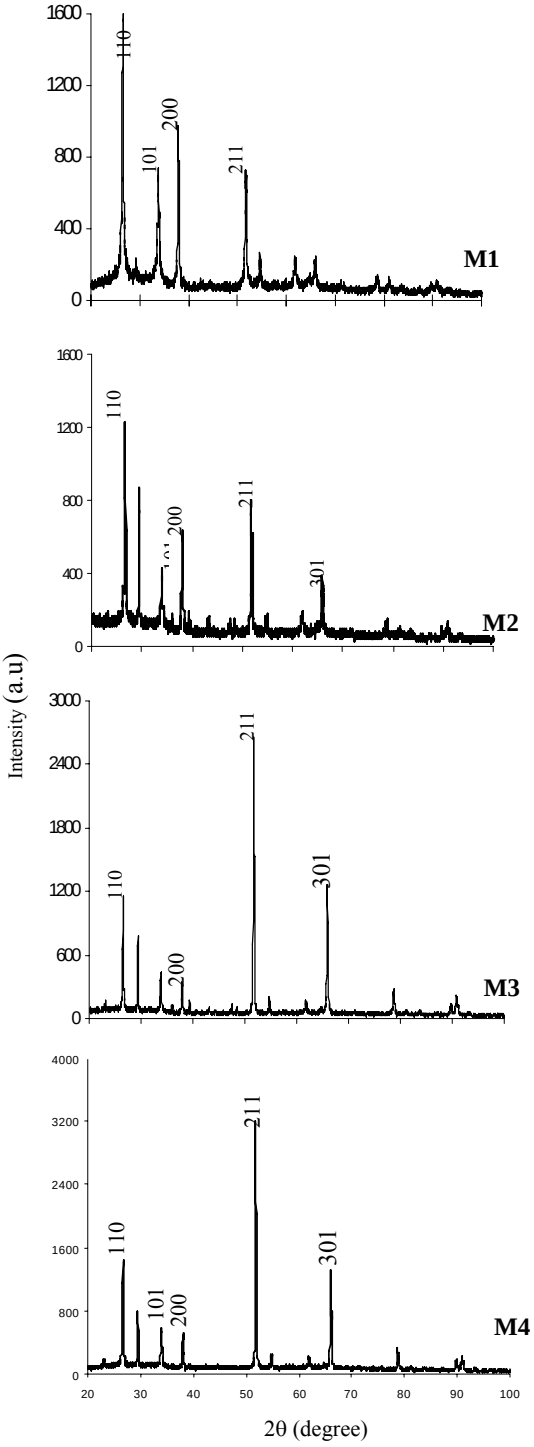

Fig. 1. The XRD patterns of SnO_2 films.

Table 1. The preferential orientations and lattice parameters of SnO_2 films.

Material	Preferential Orientation	Calculated			ASTM		
		a (Å)	b (Å)	c (Å)	a (Å)	b (Å)	c (Å)
M1	(110)	4.7460	4.7460	3.1878	4.7382	4.7382	3.1871
M2	(110)	4.7214	4.7214	3.2197	4.7382	4.7382	3.1871
M3	(211)	4.7458	4.7458	3.1875	4.7382	4.7382	3.1871
M4	(211)	4.7249	4.7249	3.1970	4.7382	4.7382	3.1871

Table 2. The half-widths (B) and grain sizes (t) of SnO_2 films.

Material	$B\times10^{-3}$ (radian)	t (nm)
M1	2.897	56
M2	2.435	67
M3	1.658	141
M4	1.580	148

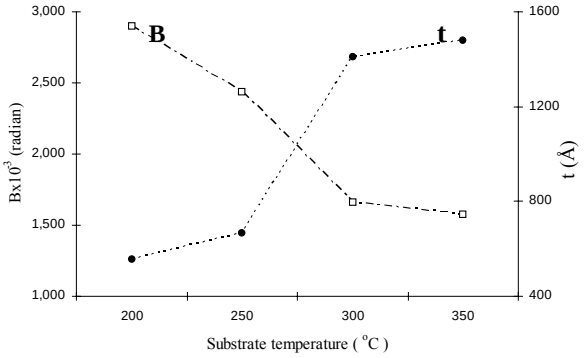

Fig. 2. The B and t values of SnO_2 films.

3.2 Surface properties

SEM micrographs were taken to investigate the surface morphologies of SnO_2 films and are shown in Fig. 3. It was determined that the surface homogeneity of the films improved with increasing substrate temperature (specially 300 and 350±5 °C). This result supports the XRD observations. Besides, SEM micrographs show different morphologies of the surface particles depending on the substrate temperature. Especially M1 and M2 films obtained at low substrate temperatures have different islands with different sizes and shapes, and their distributions on the surface are not homogeneous. But, M3 and M4 films have strong adherence to the substrates and tightly bounded particles depending on the increasing substrate temperature. These surface properties have strong effect on optical properties such as transmittance, absorbance and reflection. It is concluded that the surface properties of SnO_2 films became better for M3 and M4 films which are produced at the substrate temperatures of 300 and 350 ± 5 °C.

EDS spectra of SnO_2 films are given in Fig. 4. Sn and O elements are present in the films. Si and N elements are not expected to be in the films and may have resulted from the glass substrates. Atomic and weight percents of SnO_2 films are listed in Table 3. It was clearly seen that there are approximately one Sn atom for two O atoms, that is, SnO_2 films are almost stoichiometric.

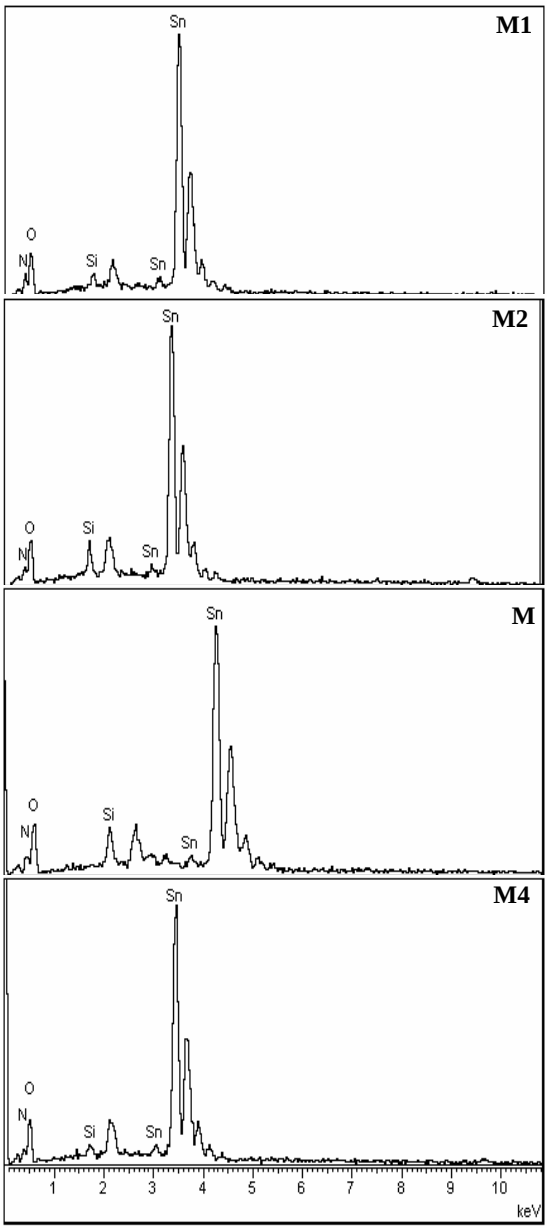

Fig. 4. The EDS spectra of SnO_2 films.

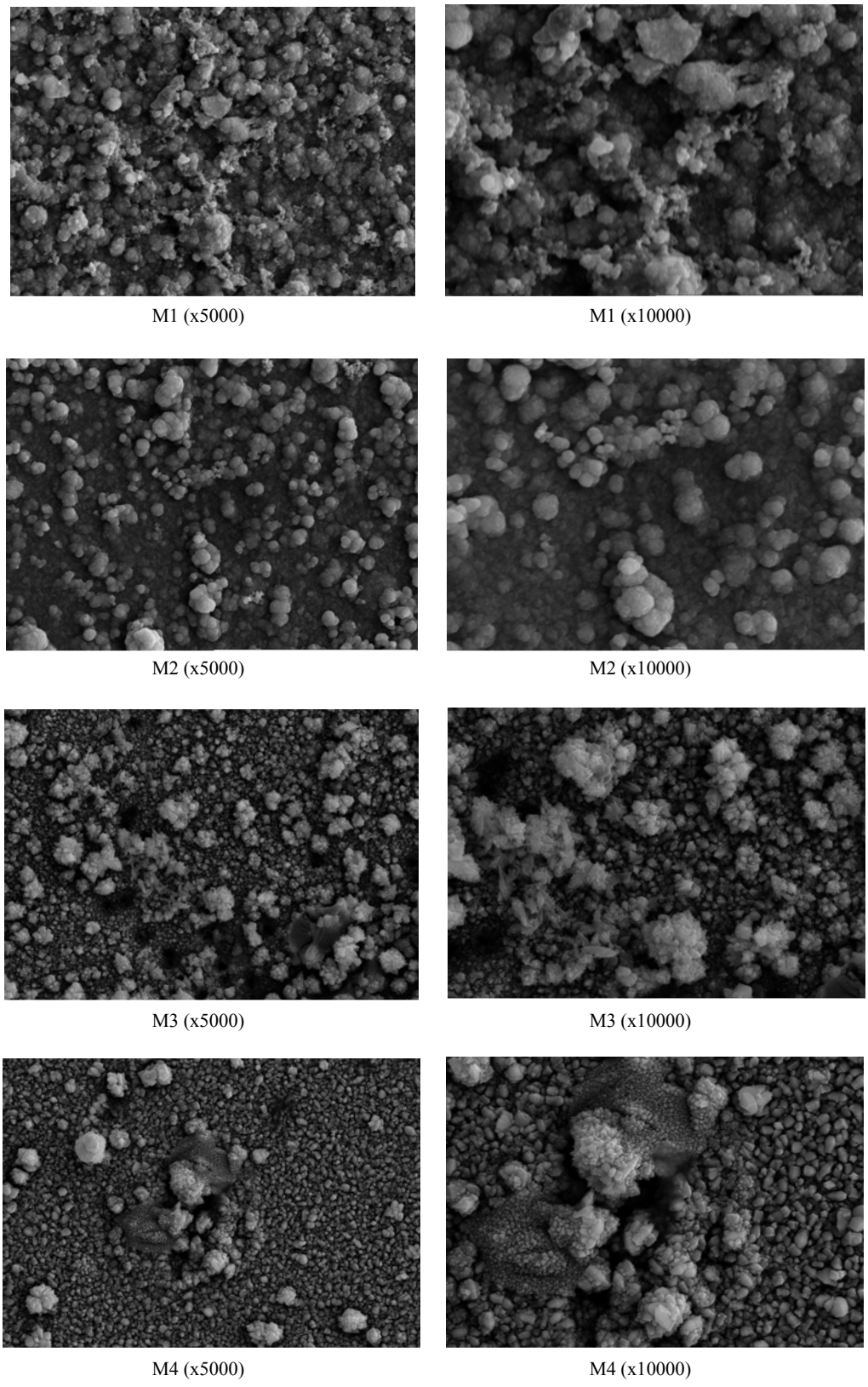

Fig. 3. The SEM micrographs of SnO_2 films.

Table 3. The EDS data of SnO_2 films.

Material	% Atom			% Elemental weight		
	Si-K	Sn-L	O	Si-K	Sn-L	O
M1	2.03	31.30	60.67	1.18	76.78	22.04
M2	4.38	28.95	66.67	2.66	74.28	23.06
M3	5.07	28.26	66.67	3.12	73.50	23.37
M4	1.28	32.05	66.67	0.73	77.53	21.74

3.3 Optical properties

The transmission spectra of SnO_2 films are shown in Fig. 5. Firstly, it was seen that the transmission values of the films are low in the visible region. We think that the low transmissions resulted from the thicknesses of the obtained films. We believe that when the thinner films are produced by changing the experimental parameters, these low transmission values will be increased. Secondly, M2 sample presented higher transmittance eventhough it is thicker than M3 and M4 films. We think that this situation is related to the crystal structure of M2 films. We think that they have high transmission values because of the cavities resulted from the very few bad crystallinization according to the M3 and M4 films. Besides, it was seen from the SEM micrographs that M3 and M4 films have better film formations on the surface. It was concluded that in these materials, the absorption values increased because of the more tightly bounded particles, thus the transmission values of the films decreased.

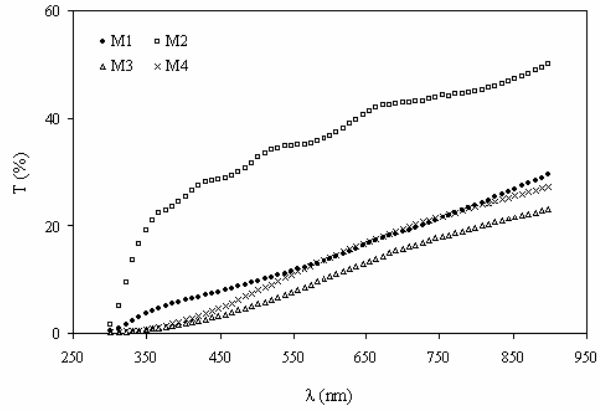

Fig. 5. The transmittance spectra of SnO_2 films.

Reflection (R), absorption coefficient (α) and refractive index (n) values of SnO_2 films were calculated using the transmittance and absorbance spectra and equations given below [39,40],

$$\alpha = \frac{A}{d} \tag{1}$$

$$R = 1 - \sqrt{Te^{A}} \tag{2}$$

$$n = \frac{1+R}{1-R} + \sqrt{\frac{4R}{(1-R)^2} - k^2} \tag{3}$$

$$k = \frac{\alpha \lambda}{4\pi} \tag{4}$$

where A is the absorbance, d is the thickness of the films, k is the extinction coefficient and λ is the wavelength of the incident light. The reflection, absorption coefficient and refractive index spectra were drawn using the calculated values. These spectra are shown in Fig. 6, 7 and 8, respectively. It was determined from Fig. 6 that the reflection values are high in the visible region. Also, the reflection values of the M2 films are low as compared to those of other films because these films have higher transmission. However, the reflection values of the M3 and M4 films did not change remarkably. The reflection properties of these films are better than those of the M2 films because M3 and M4 films have more smooth surfaces and more tightly bounded particles. It was seen from the Fig.7 that M1 and M2 films have low absorption coefficient at about 350-900 nm wavelength range, and the absorption coefficient values increased remarkably as the wavelength decreased (λ<350 nm). For M3 and M4 films, the absorption coefficient increases sharply below 550 nm and this increase is slower as compared to M1 and M2 films. It was determined that fundamental absorption regions of SnO_2 films moved to the higher wavelengths as the substrate temperature increased. The refractive index spectra of the films are shown in Fig. 8. It was seen that the refractive indexes of M1 films increase slowly with decreasing wavelength in the wavelength range of 350-900 nm and then increase sharply. Other films also have the same properties, but there is an important variation depending on the substrate temperature. That is, M3 and M4 films obtained at higher substrate temperatures have higher refractive indexes. We think that the increase of the refractive index for M3 and M4 films may be high amount of electrons. Because, when the incident light interacts with a material that has high amount of electrons, the refraction will be high, and thus the refractivity of the film will increase.

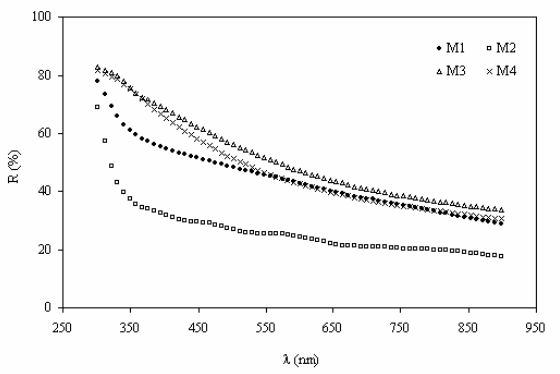

Fig. 6. The reflectance spectra of SnO_2 films.

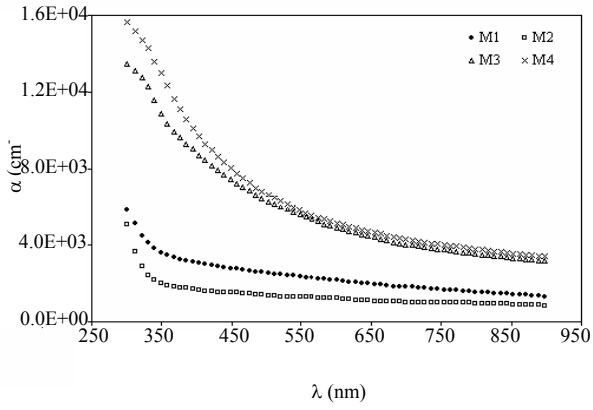

Fig. 7. The absorption coefficient spectra of SnO_2 films.

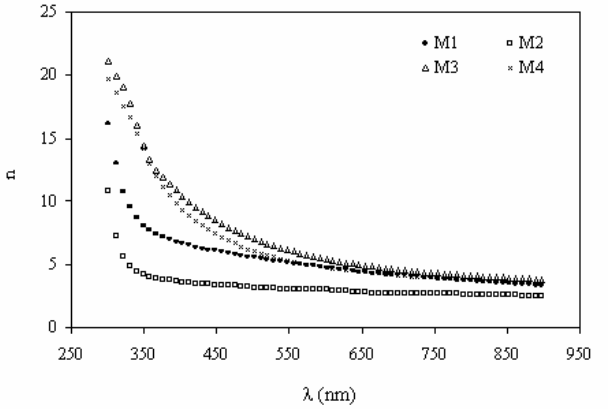

Fig. 8. The refractive index spectra of SnO_2 films.

The transmission (T), reflection (R), absorption coefficient (α) and refractive index (n) values of all films for 550 nm are given in Table 4. It was determined that the substrate temperature has a noticeable effect on the optical properties of SnO_2 films, and M2 films have the highest transmission and the lowest reflection, absorption coefficient and refractive index values.

Table 4. Some optical parameters (λ=550 nm) and band gaps (E_g) of SnO_2 films.

λ=550 nm	M1	M2	M3	M4
%T	12	35	8	11
%R	46	26	52	47
$\alpha \times 10^3$ (cm^{-1})	2.35	1.28	5.60	5.80
n	5.18	3.06	6.13	5.30
E_g (eV)	3.60	3.70	3.10	2.98

The forbidden energy gaps of SnO_2 films were determined by using optical method. The $(\alpha h\nu)^2 \sim h\nu$ plots of the films are given in Fig. 9. It was determined that all films have direct band transitions. The band gaps of the films were found between 2.98-3.7 eV and these values are given in Table 4. It was determined that the energy gaps of the M3 and M4 films obtained at high substrate temperatures are lower than those of M1 and M2 films. We can say that this is resulted from the increasing interstitial Sn atoms and/or oxygen vacancies which act as donor impurities, so extended donor impurity band becomes closer to the conduction band and maybe merges with the conduction band [41].

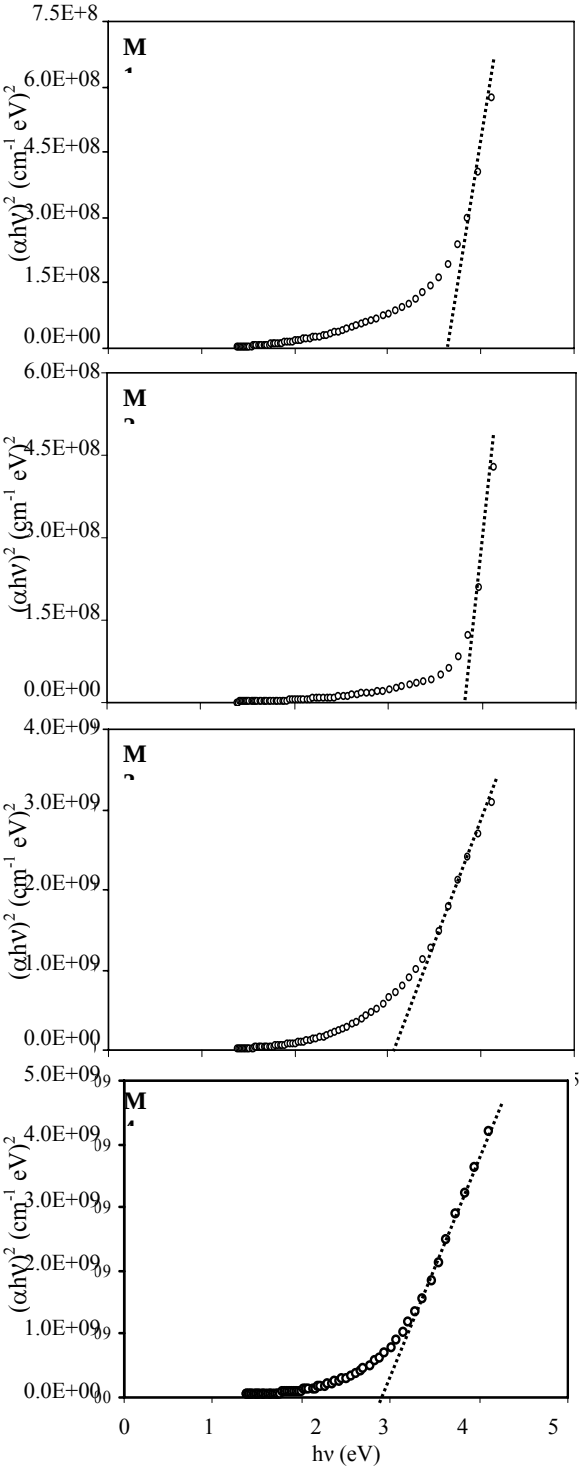

Fig. 9. $(ahv)^2 \sim hv$ graphs of SnO_2 films.

3.4 Electrical properties

The I-V characteristics of SnO_2 films were drawn in the voltage range of 0.01-10 V in dark conditions to investigate the electrical conduction mechanisms and to calculate the electrical resistivities. The I-V plots of the films on log-log scale are shown in Fig. 10. In the whole voltage range, there is a linear increase in current values with increasing voltage. So, ohmic conduction mechanism is dominant. Thus, the number of free carriers is higher than that of the injected ones from the platinum metal contact.

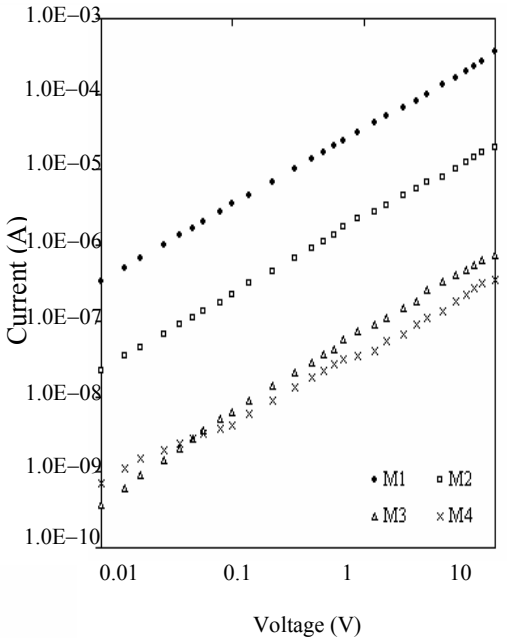

Fig. 10. The I-V characteristics of SnO_2 films.

The electrical conductivities and resistivities of SnO_2 films were calculated using two-probe technique, and these values are given in Table 5. It was seen from this table that the conductivity values changed between $5.40x10^{-1}$-$2.24x10^{-3}$ $(\Omega.cm)^{-1}$. The conductivities of the films decreased depending on the increasing substrate temperature. It was determined from XRD patterns and SEM micrographs that the structural and surface properties of the films improved with increasing substrate temperature. SnO_2 films are degenerate semiconductors, so we think that free carrier concentration of the films can increase because of the better crystallinization levels and surface morphologies. Thus, we concluded that the collision times and mobilities of the free electrons decreases since there are more conduction electrons in the structure. So, the decreasing conductivity can be explained with the diminishing mobility.

Table 5. Some electrical properties of SnO_2 films.

Material	σ $(\Omega.cm)^{-1}$	ρ $(\Omega.cm)$	E_a (meV)	E_t (eV)
M1	5.40×10^{-1}	1.85	-	0.049
M2	3.82×10^{-2}	2.62×10^{1}	2.10	0.057
M3	2.24×10^{-3}	4.46×10^{2}	-	0.082
M4	1.61×10^{-3}	6.21×10^{2}	0.28	0.063

It is well known that SnO_2 films have traps which act as donor. But the existence of the traps was not observed from the I-V plots. So, to prove the existence of the traps and to realize the general behavior of the conductivity depending on the temperature, the conductivity is plotted as a function of the temperature on a semi-logarithmic scale in the temperature range of 10-320 K. The $\ln\sigma$ vs. 1000/T plots are shown in Fig. 11. For all films, the whole temperature range was investigated in two regions. In the M1 and M3 films, the conductivity values decreased with increasing temperature in the first regions. But, conductivity of M3 films remarkably decreased as compared to M1 films. We think that in these regions for M1 and M3 films, interstitial Sn atoms and/or oxygen vacancies which act as donors ionized at low temperatures and thermal vibration energies are not sufficient to ionize the deeper donor-like traps. So, these regions represent depletion regions where shallow donors are depleted. Thus, the carrier concentration is almost constant with increasing temperature in the depletion regions. In these regions, the variation of conductivity with temperature can be explained from the variation of mobility with temperature, and the scattering by thermal lattice vibrations is the fundamental conduction mechanisms. According to the mechanism, mobility and conductivity decreases because of the thermal lattice vibrations. Thus, decreasing conductivity depending on the increasing temperature can be explained with the decreasing mobility [41]. For M2 and M4 films in the first regions, the conductivity values increased with increasing temperature. However, conductivity of M2 films remarkably increased as compared to M4 films. In the second regions conductivities increased sharply with increasing temperature for all films. We think that this variation resulted from the ionization of donor-like traps in the band gap. The activation energies of donors and the energies of donor-like traps for M2 and M4 films were calculated using the slopes of the first and second regions. For M1 and M3 films, only the energies of donor-like traps could be calculated from the slopes of the second regions because these films have depletion regions in the first regions. These energies were calculated using the equation given below,

$$\sigma = \sigma_1 \exp(-E_a / kT) + \sigma_2 \exp(-E_t / kT) \qquad (5)$$

where σ_1 and σ_2 are the pre-exponential factors, E_a is the activation energy of donors, E_t is the energy of donor-like traps and k is the Boltzmann constant [36]. This equation can be used to calculate E_a and E_t when one of the terms is neglected depending on the temperature. The activation energies of donors and the energies of donor-like traps are listed in Table 4. It was seen that the activation energies of M4 films are smaller than those of the M2 films. We think that this result arose from the higher number of interstitial Sn atoms and/or oxygen vacancies which act as donors in M4 films. Donor levels split to sub-energy levels because of the high donor concentration and so, donor impurity band is formed [41]. Thus, the activation energies of donors for M4 films decreased because the extended donor impurity band becomes closer to the conduction band. It was also seen from Table 5 that there was not a regular variation in the E_t values of the films with increasing substrate temperature. So, we think that both the number and the distribution of donor like traps in the band gap changed with substrate temperature.

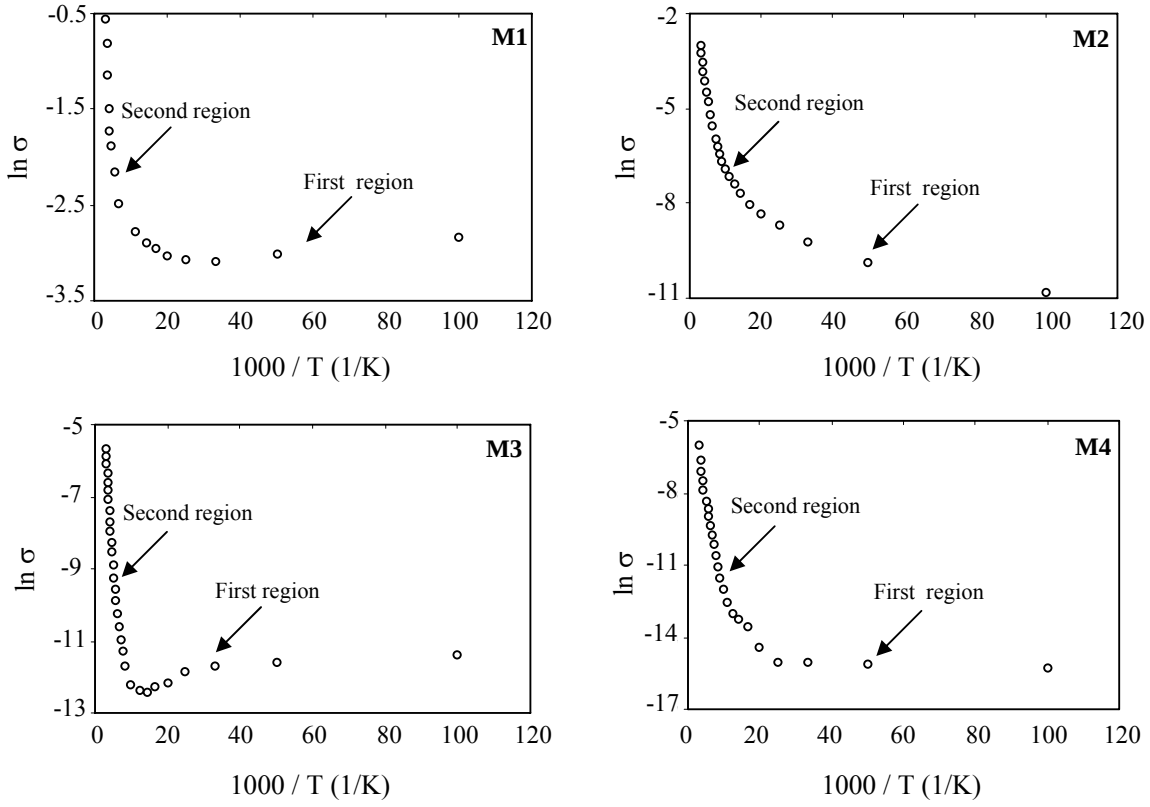

Fig. 11. The lnσ~1000/T graphs of SnO_2 films.

The electrical conductivity types of SnO_2 films were determined to be n-type using hot-probe technique. It is an expected situation because these films have interstitial Sn atoms and/or oxygen vacancies which act as donors.

4. Conclusions

In this work SnO_2 films were obtained by USP technique, and the effect of substrate temperature on structural, surface, optical and electrical properties was investigated. It was determined from the structural analyses that the substrate temperature has a strong effect on the structural properties, and the crystallinity levels of SnO_2 films improved with increasing substrate temperature. It was determined from SEM investigations that the effect of increasing substrate temperature was to decrease the surface roughening and change strongly the morphologies of SnO_2 films. Also, the films have strong adherence to the substrates and more tightly bounded particles depending on the increasing substrate temperature. EDS analyses showed that Sn and O elements are present in the films and SnO_2 films are almost stoichiometric. The transmittance values of SnO_2 films are low because of the thicknesses, and M2 films have the highest transmission and the lowest reflection and absorption coefficient values. We believe that when the thinner films are produced by changing the experimental parameters, they will have higher transmission. Also, it was determined from optical investigations that the band gaps of the films were between 2.98-3.70 eV, and energy gaps of the M3 and M4 films obtained at high substrate temperatures decreased as to M1 and M2 films. It was concluded that this is resulted from the increasing

interstitial Sn atoms and/or oxygen vacancies, so extended donor impurity band became closer to the conduction band and maybe merged with it [41]. Electrical investigations showed that all films have ohmic conduction mechanisms, and the conductivities of the films changed between $5.40x10^{-1}$-$2.24x10^{-3}$ $(\Omega.cm)^{-1}$. The conductivity values were decreased depending on the increasing substrate temperature. We concluded that the mobilities of the free electrons decreased because of the high number of conduction electrons in the structure. So, the decreasing conductivity can be explained with the mobility. It was seen from the conductivity-dependent temperature analyses that donor impurity band is formed in the films because of the high donor concentration. Also it is concluded that the number and the distribution of donors and donor-like traps in the band gap changed with substrate temperature. It can be concluded from all investigations that substrate temperature has a strong influence on the structural, surface, optical and electrical properties of SnO_2 films, and M2 films can be used as window materials and transparent contacts in photovoltaic solar cells because of the high electrical conductivities and transmissions.

References

[1] O. Madelung, Semiconductors-basic data, Springer-Verlag Berlin Heidelberg, Germany, (1996).
[2] D. Briand, M. Labeau, J. F. Currie, D. Delabouglise, Sensors and Actuators B **48**, 395 (1998).
[3] Y. J. Lin, C. J. Wu, Surface and Coatings Technology **88**, 239 (1996).
[4] F. M. Amanullah, K. J. Pratap, V. H. Babu, Materials Science and Engineering B **52**, 93 (1998).
[5] F. Yubero, V. M. Jimenez, A. R. G. Elipe, Surface Science **400**, 116 (1998).
[6] S. A. Pianaro, P. R. Bueno, P. Olivi, E. Longo, J. A. Varela, Journal of Materials Science: Materials in Electronics **9**, 159 (1998).
[7] T. M. Racheva, G. W. Cnitchlow, Thin Solid Films **292**, 299 (1997).
[8] J. M. Laurent, A. Smith, D. S. Smith, J. P. Bonnet, R. R. Clemente, Thin Solid Films **292**, 145 (1997).
[9] C. Terrier, J. P. Chatelon, J. A. Roger, Thin Solid Films **295**, 95 (1997).
[10] K. Y.Rajpure, M. N. Kusumade, M. N. N. Spallart, C. H. Bhosale, Materials Chemistry and Physics **64**, 184 (2000).
[11] Z. B. Zhou, R. Q. Cui, Q. J. Pang, Y. D. Wang, F. Y. Meng, T. T. Sun, Z. M. Ding, X. B. Yu, Applied Surface Science **172**, 245 (2001).
[12] J. Isidorsson, C. G. Granqvist, Solar Energy Mater. Solar Cells **44**, 375 (1996).
[13] K.L. Chopra, S. Major and D.K. Pandya, Thin Solid Films **102**, 1 (1983).
[14] C.G. Granqvist, Handbook of Inorganic Electronic Materials, Elsevier Publication, The Netherlands. (1995).
[15] B. Stjerna, E. Olsson, C. G. Granqvist, J. Appl. Phys. **76**, 3797 (1994).
[16] V. Vasu, A. Subrahmanyam, Thin Solid Films **193-194**, 973 (1990).
[17] C. Li, B. Hua, Thin Solid Films **310**, 238 (1997).
[18] S. Rani, S. C. Roy, M. C. Bhatnagar, Sensors and Actuators B, (2006), in press.
[19] Y. Hu, S.H. Hou, Materials Chemistry and Physics **86**, 21 (2004).
[20] M. S. Wagh, L. A. Patil, T. Seth, D. P. Amalnerkar , Materials Chemistry and Physics **84**, 228 (2004).
[21] P. Ifeacho, T. Huelser, H. Wiggers, C. Schulz, P. Roth, Proceedings of the Combustion Institute, (2007), in press.
[22] B. J. Lokhande, D. Uplane, Appl. Surf. Sci. **167**, 243 (2000).
[23] D. R. Acosta, E. P. Zironi, E. Montoya, W. Estrada, Thin Solid Films **288**, 1 (1996).
[24] T. Schuler, M. A. Aegerter, Thin Solid Films **351**, 125 (1999).
[25] D. J. Goyal, C. Agashe, M. G. Takwale, B. R. Marethe, V. G. Bhide, Journal of Materials Science **27**, 4705 (1992).
[26] A. S. Riad, S. A. Mahmoud, A. A. Ibrahim, Physica B, **296**, 319 (2001).
[27] D. F. Paraguay, L. W. Estrada, N. D. R. Acosta, E. Andrade, and M.M.Yoshida, Thin Solid Films 350, 192 (1999).
[28] N. Benramdane, W. A. Murad, R. H. Misho, M. Ziane, Z. Kebbab, Materials Chemistry and Physics **48**, 119 (1997).
[29] B. Thangaraju, Thin Solid Films **402**, 71 (2002).
[30] F. İzci, S. Köse, Turkish Journal of Physics **21**, 1043 (1997).
[31] I. Taniguchi, D. Song, M. Wakihara, Journal of Power Sources **109**, 333 (2002).
[32] A.K. Ivanov-Schitz, A.V. Nistuk, N.G. Chaban, Solid State Ionics **139**, 153 (2001).
[33] F. Atay, S. Kose, V. Bilgin, I. Akyuz, Materials Letters **57**, 3461 (2003).
[34] F. Atay, V. Bilgin, I. Akyuz, S. Kose, Materials Science in Semiconductor Processing **6**, 197 (2003).
[35] V. Bilgin, S. Kose, F. Atay, I. Akyuz, Materials Letters **58**, 3686 (2004).
[36] V. Bilgin, S. Kose, F. Atay, I. Akyuz, Journal of Materials Science **40**, 1909 (2005).
[37] A. S. Riad, S. A. Mahmoud, A. A. Ibrahim, Physica B **296**, 319 (2001).
[38] B. D. Cullity, The Elements of X-Ray Diffraction, second ed., Addison-Wesley, Reading, MA, (1978).
[39] H. Kim, A. Pique, J.S.Horwitz, P.Murata, Z. H.Kafafi,C.M.Gilmore and D.B.Chrisey, Thin Solid Films **377-378**, 798 (2000).
[40] S. H. Brewer, S. Franzen, Journal of Alloys Compounds **338**, 73 (2002).
[41] A. Polyakov, Semi-conductors made simple, Mir Publishers Moscow, Russian 240 p, (1985).

*Corresponding author: fatay@ogu.edu.tr